

# Modélisation, Simulation multi-niveau pour l'optimisation de politiques de vaccination

October 27, 2014

**Phd: TRAN Thi Cam Giang**

**Thesis direction: Yann Chevalere (PR, Université Paris 13), Jean-Daniel Zucker (DR1, UMI UM-MISCO, IFI-MSI, IRD)**

**Co-supervision: Marc Choisy (CR1, MIVEGEC, NIHE, IRD)**

## 1 Introduction

This thesis is taking place in a context where many public health serious events have occurred in the world : SRAS in 2003, avian influenza in 2004 or swine flu in 2009. In particular, in the start of the 2014, the World Health Organization (WHO) had officially to state global measles epidemic outbreak. In the first three months of the year 2014, there were about 56,000 cases of measles infections in 75 countries [20], in particular in southeast Asia particularly, in Vietnam [9]. This has pointed out the important role of the epidemiological phenomena anticipation when diseases occur. Moreover, for vaccination policies, the mass policy (vaccinate the maximum number of children before certain age) is the oldest (started from the 1950s in the rich countries) and is now the most used. The problem of this vaccination policy is too expensive, ineffective and quite impossible to implement in poor countries, especially in Africa as both financial and logistical problems. (e.g. the WHO project “Extended Programm on Immunization” in Vietnam for the measles extinction before 2012 is failed). In addition, when a vaccination policy is performed in a country, there is only one policy, but in modelation, we can realize many policies and at the same time estimate them. Therefore, optimize the vaccination policies in Artificial Intelligence in order that these policies may become more effective, less expensive, and take into account the spatial dimension, is the goal of this thesis.

To carry out this goal, the first task is to make a state of the art covering the different epidemic models being used in the field of epidemiological modeling. In the second step, we will focus on design or expanse for representation language that allows modelers to express the goals of model simulations as well as constraints related to them. In the third step, we will concetrare on stochastic models, and investigate disease spread characteristics between population and community in a spatial context. We then study local/global disease persistence, disease periodicity and the influence of space on the disease persistence. Finally, we will perform vaccination policies in a metapopulation and optimize them bu using reinforcement learning algorithms

## 2 Epidemic models

### 2.1 Epidemic model

It is known that, there are many current models that are used to model complex systems in nature, in ecology system and in epidemiology. Mathematical models in epidemiology are a typical exemple. These models permit us to present behavior of diseases and disease process in mathematics. They have given us good results in mathematics as deterministic models in which every set of variable states is only determined by parameters in the model and by sets of previous states of these variables. In detail, the deterministic models are equations, for that they perform the same way for a given set of initial conditions. But they don't have randomness, dynamics, and don't present dynamic of diseases in nature. Thus, stochastic models have been proposed. A sotchastic model is always more realistic than a deterministic one. These models have stochastic and variable states are not described by unique values, but by

probability distributions. It is reason for that, we will use the stochastic models to predict extinction propability of disease in spatial context[14].

To present the process of infection propagation in community, we give here the development of epidemic models by focusing on acute infections, assuming the pathogen causes illness for a periods of time followed by (typically lifelong) immunity. The first simplest model is the **S-I-R** model created by W. O. Kermack and A. G. McKendrick in 1927. The authors categorized hosts within a population as **S**usceptible (if not yet exposed to the pathogen), **I**nfectious (if currently infected by the pathogen) and **R**ecovered (if they have successfully cleared the infection). From the simplest SIR model, in order to accord each infectious disease and real property of disease, scientists have modified it, made it different multiforme. However, in shape of this thesis, we concentrate on the SEIR model (as the figure 1) that fit many currently infectious diseases in the world. Each patient must pass four steps : susceptible stage, incubation stage, infectious stage and recovered stage.

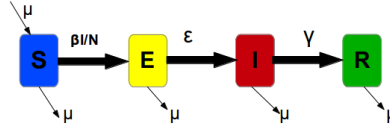


Figure 1: SEIR model

In this model, the host population ( $N$ ) is divided into four classes : susceptible  $S(t)$ , exposed  $E(t)$ , infected  $I(t)$  and recovered  $R(t)$ . We have :

$$N(t) = S(t) + E(t) + I(t) + R(t)$$

- Classe  $S(t)$  : contains the number of individuals not yet with the disease at time  $t$ , or those susceptible to the disease.
- Classe  $E(t)$  : contains the number of individuals who are in the exposed or latent period of the disease.
- Classe  $I(t)$  : contains the number of individuals who have been infected with the disease and are capable of spreading the disease to those in the susceptible category.
- Classe  $R(t)$  : contains the number of individuals who have been infected and then removed from the disease, either due to immunization or due to death. Individuals of this class are not able to be infected again or to transmit the disease infection to others.

The conceptual descriptions of the model can be represented by a flow diagram above. The flow diagram for the SEIR model uses arrows to present the movement between the S and I classes, the E and I classes and the I and R classes. Here, individuals are born susceptible, die at a rate  $\mu$ , become infected with the force of infection  $\lambda$  that is a function among the contact rate  $\beta$ , the number of infected individual  $I$  and the population size  $N$ , infectious after a latency period of an average duration of  $1/\sigma$  and recover at the rate  $\gamma$ .

## 2.2 Process stochasticity

In the process stochasticity, we talk about demographic and environmental stochasticities in epidemic models. The demographic stochasticity is strongly controlled by population size such as the birth and death rates, contamination, etc. But, the environmental stochasticity is just affected by environmental factors what we can not govern. Therefore, there are many epidemic models that focus on exploration of demographic stochasticity.

Demographic stochasticity is considered as fluctuation in population processes that are based the random nature of events at the level of the individual. Each event is related to one baseline probability fixed, individuals are presented in differing fates due to chance. In addition to the demographic stochasticity, the number of infectious, susceptible, exposed and recovered individuals is now required to be an interger. Modeling approaches that incorporate demographic stochasticity are called event-driven methods. These methods require explicit consideration of events. The first method "First Reaction Method" is born in 1976 by Gillespie. Then, according to this first method and these two key factors of demographic stochasticity models (event, randomness) , many scientists have improved the first method,

and created many better algorithms for stochastic simulations. There are two main types of methods, exact methods and approximative methods. The typical approach in exact methods most practitioners use, is the algorithm “Direct Method” of Gillespie(1977) improved from the first approach “First Reaction Method”, and in approximative methods, is the “tau-leaping” method.

For the Direct Method (Gillespie 1977), the first step estimates the time until the next event, by cumulating the rates of all possible events. Then, by transforming event rates into probabilities, the method randomly selects one of these events. The time and numbers in each class are then updated according to which event is chosen. We repeat this process to iterate model through time.

For the “tau-leaping” method, the main crux is the use of Poisson random variables to approximate the number of occurrences of each type of reaction event during a carefully selected time period,  $\tau$ .

According to these two types of algorithms, the common point is both methods use continuous-time Markov process for which the transition rates are constants, isn’t a function of time. The future state of the process, is only conditional on the present state, but independent of the past.

However, for the exact algorithm, its advantage give us a really exact approach to simulate time-to-event model. This process is repeated to iterate the model. Gibson & Bruck(2000) [14] modified the first reaction method and created the Next Reaction method that substantially more challenging to program but is significantly faster than even the method when there are a large number of different event types. The Direct, First Reaction and Next Reaction methods are all exact stochastic approaches of the underlying ordinary differential equations. But, its disadvantages are 1) noise in exact simulations only affects the probabilities associated with fates of individuals and the updating of each consecutive event is independent – there is no assumption concerning environmental stochasticity; 2) these exact solutions become too slow and impractical when any one transition rate is large, when there is a big number of subpopulations or one a big number of event in a metapopulation. It is the reason for that, approximate models have been proposed instead of the exact stochastic methods. Gillespie (2001) has proposed a new method that decreases the simulation accuracy, but increases simulation speed. This is the “tau-leap method” known as an approximate method reduces the number of iterations by treating transition rates as constant over time periods for which this approximation leads to little error [14] as mentioned above. However, when we use the “tau-leap method”, there is a possibility, the number of individual in each class can become negative. View the figure about simulation speed of methods 2[14].

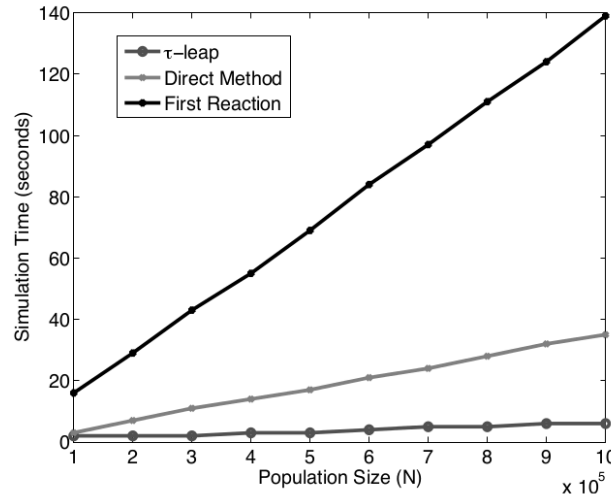


Figure 2: Figure is extrait from Keeling (2008) The time (in seconds) to simulate 1000 years of SEIR epi- demics ( $\mu = 0.02$  per year,  $1/\sigma = 8$  days,  $1/\gamma = 10$  days) on a 3.4GHz Pentium PC. For Gillespie’s Direct (light grey line) and First Reaction (black line) methods, as the population size increases so does the simulation time, which, for very large populations, could become prohibitive. In contrast, the “ $\tau - leap$ ” method (dark grey) is fast and largely unaffected by population size [14].

According this figure 2, when the population size increases, the simulation time of the three methods (First Reaction, Direct Method,  $\tau - leap$ ) is almost augmented. The simulation time of the method “First Method” is maximum, it means that this is the slowest method, but the simulation time of the method “ $\tau - leap$ ” is minimum or the fastest.

In the shape of my thesis, we will use the direct method to exactly estimate spread of diseases in metapopulation. Because the direct method is one exact approach and its simulation time isn't too slow and too fast. Afterward, we will use the approximate method to explore vaccination policies.

### 3 Approaches in use

#### 3.1 Deterministic model for many cities

##### 3.1.1 Deterministic model for many cities

In modeling of ecological system, presenting interactions between humans, subpopulations and geographic conditions, the metapopulation model is a good choice. Metapopulation is a set of subpopulations with mutual interaction [15] here a subpopulation can only go extinct locally and be recolonized by another after it is emptied by extinction [4, 7, 15]. In the epidemic models, the standard SEIR model (susceptible-exposed-infective-recovered) has been strongly developed for the dynamics of directly infectious disease [3]. For disease-based metapopulation models, we give here a suitable new version of the SEIR equation that would be as follows:

Consider a metapopulation of  $n$  sub-populations. In a subpopulation  $i$  of size  $N_i$ , disease dynamics can be deterministically described by the following set of differential equations [2]:

$$\frac{dS_i}{dt} = \mu N_i - \lambda_i S_i - \mu S_i \quad (1)$$

$$\frac{dE_i}{dt} = \lambda_i S_i - \mu E_i - \sigma E_i \quad (2)$$

$$\frac{dI_i}{dt} = \sigma E_i - \mu I_i - \gamma I_i \quad (3)$$

$$\frac{dR_i}{dt} = \gamma I_i - \mu R_i \quad (4)$$

where  $S_i$ ,  $E_i$ ,  $I_i$  et  $R_i$  are the numbers of susceptible, exposed, infectious and recovered in this sub-population  $i$  respectively. Individuals are born susceptible, die at a rate  $\mu$ , become infected with the force of infection  $\lambda_i$ , infectious after a latency period of an average duration of  $1/\sigma$  and recover at the rate  $\gamma$ .

##### 3.1.2 Formula for force of infection

The force of infection depends not only on the total population size  $N_i$  and the number of infected  $I_i$  in subpopulation  $i$ , but also in other sub-populations [14].

$$\lambda_i = \beta_i \frac{I_i}{N_i} + \sum_{\substack{j=1 \\ j \neq i}}^n \rho_{ij} \left[ \frac{\beta_i [(1 - \varepsilon_{ij}) I_j - I_i]}{N_i} + \frac{\varepsilon_{ij} \beta_j I_j}{N_j} \right] \quad (5)$$

where  $\beta_i$  is the contact rate in population  $i$  and  $\rho_{ij} = \rho_{ji}$  ( $0 \leq \rho_{ij} \leq 1$  and  $\rho_{ii} = 1$ ) is the coupling between subpopulations  $i$  and  $j$ . Among the infections caused by contacts with infected from other subpopulations,  $\varepsilon_{ij} = \varepsilon_{ji}$  ( $0 \leq \varepsilon_{ij} \leq 1$ ) is the proportion of infections due to susceptible individuals visiting other populations as opposed to infected individuals from other populations visiting the focal population. See appendix for detail on the construction of this equation. We can verify that in the limit case on one single subpopulation in the metapopulation ( $i = j$  and  $n = 1$ ) we have

$$\lambda_i = \beta_i \frac{I_i}{N_i}. \quad (6)$$

Consider that the contact rate  $\beta_i$  is seasonally forced [1] and seasonality is an annually periodic function of time [6]. As a result,

$$\beta_i(t) = b_0 \left[ 1 + b_1 \cos \left( \frac{2\pi t}{T} + \varphi_i \right) \right] \quad (7)$$

where  $t$  is the time,  $b_0$  and  $b_1$  are the mean value and amplitude of the infection rate  $\beta$  at which susceptible individuals become infected,  $T$  and  $\varphi_i$  are the period and the phase of the forcing. With the annual sinusoidal form of the infection rate, we really have the sinusoidally forced SEIR metapopulation model.

### 3.1.3 Equilibrium values of the system

In a case the infectious contact rate is constant, the equilibrium values of the variables  $S$ ,  $E$ ,  $I$  and  $R$  can be expressed analytically as follows. We know that, in simulation, the equilibrium state allow a disease to persist in a population for a long time. So, an infectious disease in the *subpopulation<sub>i</sub>* is available in long term this system is at equilibrium. It means that at which  $\frac{dS_i}{dt} = \frac{dE_i}{dt} = \frac{dI_i}{dt} = \frac{dR_i}{dt} = 0$  (\*). Thus, we let all equations (equations 1 - 4) in the system be equal to zero, then calculate the values of the variables (now denoted by  $S_i^*$ ,  $E_i^*$ ,  $I_i^*$ , and  $R_i^*$ ) that satisfy this condition (\*). We have these values as follows:

$$S_i^* = N_i \frac{(\gamma + \mu)(\sigma + \mu)}{\beta\sigma} \quad (8)$$

$$E_i^* = N_i \mu \left( \frac{1}{\sigma + \mu} - \frac{\gamma + \mu}{\beta\sigma} \right) \quad (9)$$

$$I_i^* = N_i \mu \frac{\beta\sigma - (\sigma + \mu)(\gamma + \mu)}{\beta(\sigma + \mu)(\gamma + \mu)} \quad (10)$$

$$R_i^* = N_i - S_i^* - E_i^* - I_i^* \quad (11)$$

Here, if we set  $R_0 = \frac{\beta\sigma}{(\gamma + \mu)(\sigma + \mu)}$ , so we have

$$S_i^* = N_i \frac{1}{R_0} \quad (12)$$

$$E_i^* = N_i \frac{\mu\sigma}{R_0} (R_0 - 1) \quad (13)$$

$$I_i^* = N_i \frac{\mu}{\beta} (R_0 - 1) \quad (14)$$

$$R_i^* = N_i - S_i^* - E_i^* - I_i^* \quad (15)$$

One nomal conditions for all population availabes is that the equilibrium values cannot be negative. Therefore, an infectious disease is available in the *subpopulation<sub>i</sub>* if  $R_0 > 1$ . Now, the endemic equilibrium in the system is given by  $(S_i^*, E_i^*, I_i^*, R_i^*) = (N_i \frac{1}{R_0}, N_i \frac{\mu\sigma}{R_0} (R_0 - 1), N_i \frac{\mu}{\beta} (R_0 - 1), N_i (1 - \frac{1}{R_0} - \frac{\mu\sigma}{R_0} (R_0 - 1) - \frac{\mu}{\beta} (R_0 - 1)))$ .

## 3.2 Stochastic model for many subpopulation in a metapopulation

### 3.2.1 Random number generator

Random numbers have a big role in aplications such as simulation, game-playing, statistical sampling, transport calculations and computations in satistical physics. Depending on each appication, it has its own generator with its own set of advantages and disadvantages. In the shape of my thesis, we use the pseudo-random number generators (PRNGs) in the programming language C++. This is an algorithm that can automatically create long runs of numbers with good random properties. The sequence of values generated by the algorithms is generally determined by a fixed number called a “seed”. However, there is a problem is if the number of time that call generator is too large, so the sequence of values repeats or the memory usage grows without bound. In addition to the set of the random number generators, here we mention also a method that generates random variables with a normal distribution (i.e. Gaussian) of C. Paciorek in 2001. This method allows us to generate a standard normally-distributed random variable (scalar) due to the Gaussian distribution. We will use both generators to do simulations.

### 3.2.2 Stochastic model for many subpopulations in a metapopulation

In order to study the persistence of the disease, we must consider a stochastic version of the model [13, 16, 17]. We use for that a population-based time-to-next-event model based on Gillespie’s algorithm [5]. Table 1 lists all the events of the model, occurring in subpopulation  $i$ .

Table 1: Events of the stochastic version of the model of equations 1-4, occuring in subpopulation  $i$ .

Events	Rates	Transitions
birth	$\mu N_i$	$S_i \leftarrow S_i + 1$ and $N_i \leftarrow N_i + 1$
death of a susceptible	$\mu S_i$	$S_i \leftarrow S_i - 1$
death of an exposed	$\mu E_i$	$E_i \leftarrow E_i - 1$
death of an infected	$\mu I_i$	$I_i \leftarrow I_i - 1$
death of an immune	$\mu R_i$	$I_i \leftarrow I_i - 1$
infection	$\lambda_i S_i$	$S_i \leftarrow S_i - 1$ and $E_i \leftarrow E_i + 1$
becoming infectious	$\sigma E_i$	$E_i \leftarrow E_i - 1$ and $I_i \leftarrow I_i + 1$
recovery	$\gamma I_i$	$I_i \leftarrow I_i - 1$ and $R_i \leftarrow R_i + 1$

## 4 Result

### 4.1 Experiences

Here, in order to do simulation, in first steps of my thesis, we focus on the exploration of the influence of the phase difference among subpopulations, the population size, number of subpopulation in a metapopulation, couplage strength between two subpopulations on the persistence of infectious diseases in spatial structure. The number of subpopulation in a metapopulation is in the interval from 2 to 30. The population size of each subpopulation is from 5000 individuals to 500000 individuals. Finally, the couplage strength is from 0.0001 to 1.0. In the next part, we will show results obtained.

### 4.2 Package "dizzys" for stochastic SEIR metapopulation model

We built successfully a package named "dizzys". This package in R implements both the exact and approximate methods for the deterministic/stochastic SEIR/SIR models by integrating the R package and the C++ implementation. We use C++ to perform the algorithms, and use R to create interfaces. Hence, this new integration is faster than any pure R implementation. The figures below are results of the simulations of deterministic and stochastic SEIR models. View the figure ??.

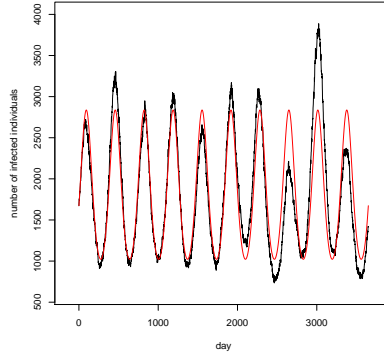


Figure 3: Result of deterministic model and stochastic model with  $N=10^7$ ,  $\mu = 1/(70 * 365)$  per day,  $\beta_0 = 1250/365$  day,  $\beta_1 = 0.1$  day,  $1/\sigma = 8$  days,  $1/\gamma = 5$  days,  $\varphi = 0$  rad, simulation time = 10 years. The red curve is for the deterministic model. The black curve is for the stochastic model.

The result (figure 3) is a good result. The deterministic curve is so close to the stochastic model. This figure points out that we have successfully transformed the deterministic model to the stochastic model.

Then, we simulate a metapopulation of three subpopulation with  $N=10^7$ .

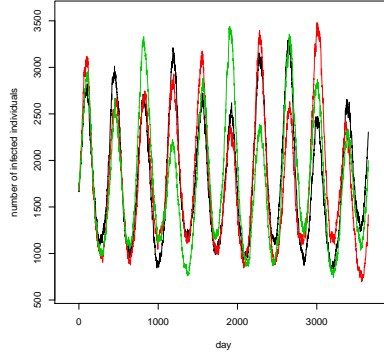


Figure 4: Simulation of a metapopulation of three subpopulations with  $N=10^7$ ,  $\mu = 1/(70 \times 365)$  per day,  $\beta_0 = 1250/365$  per day,  $\beta_1 = 0.1$  per day,  $1/\sigma = 8$  days,  $1/\gamma = 5$  days,  $\varphi_1 = \varphi_2 = \varphi_3 = 0$  rad, coupling rate  $\rho = 0.0$  and simulation time = 10 years. The curve of each subpopulation fluctuates very close to each other with the same all values of parameters and initial availables.

### 4.3 Global persistence in a metapopulation

Here, we start exploiting the package "dizzys". In order to illustrate the interaction between disease transmissibility and phase difference among subpopulations. We start this section by studying the stochastic SEIR model in a metapopulation of  $n$  subpopulations. For this meta-population, we observe the disease extinction in time due to spatial synchrony or spatial asynchrony that are influenced by phase difference in seasonal forcing parameter. To create phase difference, we change the value of the forcing phase for each city. In this experience, we use a parameter  $\varphi_{max}$  in radian that runs in the interval from zero to  $\pi$ . With each value of  $\varphi_{max}$ , based on  $n$  the number of subpopulations in the metapopulation, we divide the interval  $[0, \varphi_{max}]$  into a set of  $(n-1)$  equal samples, so the value of the forcing phase of the  $i^{th}$  city is correspondent to  $i^{th}$  value in the set. We call  $\varphi_{max}$  asynchrony parameter.

For our metapopulation of  $n$  subpopulations, to do so we run first  $m$  independent simulations of our stochastic model. We calculate then the average metapopulation size by summing subpopulations at each sample time and averaging across the entire time series for each metapopulation. Lastly, we record the dates  $t$  of global disease extinction in all these  $m$  metapopulations. These dates allowed to draw Kaplan-Meier survival curves from which we estimated the extinction rate  $\chi$ :

$$M(t) = \exp(-\chi t) \quad (16)$$

where  $M(t)$  ( $0 \leq M(t) \leq m$ ) is the number of metapopulations in which the disease is not extinct at time  $t$ . The extinction rate  $\chi$  is reparameterized in terms of predictor variables and regression parameters. Here, we reparameterize  $\chi$  with  $\chi = \exp(-p)$  where  $p$  is a parameter that characterizes the probability of the global disease persistence and is estimated by the survival regression model (R package 'survival' [19]). For that, we find the extinction rate where the number of metapopulations in which the disease is extinct in time. Then, we will study the relation between the global persistence and its level of synchrony due to the phase of the forcing.

#### 4.3.1 Global persistence and time

Here, we start with a simplest metapopulation of two subpopulation. We have  $N_1 = N_2 = 300,000$ , the rate of coupling  $\rho = 0.01$ , the simulation time 50 years, the number of simulations  $m = 100$ , and  $\varphi_{max} = \{0, \pi/2, \pi\}$ . We have three Kaplan-Meier survival curves for each value of  $\varphi_{max}$  as figure 5.

The phase of forcing of the *subpopulation*<sub>1</sub> is always fixed 0, but this of the *subpopulation*<sub>2</sub> increases from 0 to  $\pi$ . It means that, in the first experience,  $\varphi_{max} = 0$ , the two subpopulations are in synchrony with all beginning conditions. The disease persistence time is the shortest. Then, the two subpopulations become asynchrony when  $\varphi_{max} = \pi/2$  or  $\pi$ . The symmetry of fixed points is just broken at the starting moment. It is reason for that the level of synchrony of the metapopulation decreases. Additionally, we find that the value of the asynchrony parameter  $\varphi_{max}$  change according to increasing tendency, the phase difference between the fluctuations of the two infection rates  $\beta$  increases also, and the global persistence time in the metapopulation thus augments. When  $\varphi_{max} = \pi$ , the two subpopulations are in

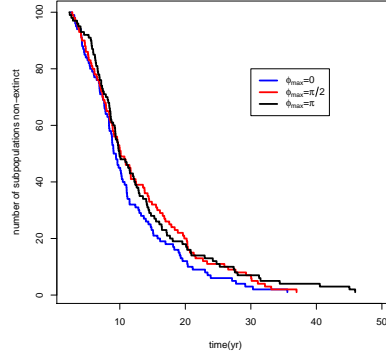


Figure 5: Kaplan-Meier survival curves for disease persistence after 100 different simulation, with  $N=300000$ ,  $\mu = 1/(70 * 365)$  per day,  $\beta_0 = 1250/365$  per day,  $\beta_1 = 0.1$  per day,  $1/\sigma = 8$  days,  $1/\gamma = 5$  days, coupling rate  $\rho = 0.01$ . Disease persistence time after 100 simulations of  $\varphi_{max} = 0$  rad,  $\varphi_{max} = \pi/2$  rad and  $\varphi_{max} = \pi$  rad. The blue survival curve for  $\varphi_{max} = 0$ , the red survival curve for  $\varphi_{max} = \pi/2$  and the black curve for  $\varphi_{max} = \pi$ . The persistence time of  $\varphi_{max} = 0$  is the shortest. The persistence time of  $\varphi_{max} = \pi$  is the longest.

antiphase. This is the most difficult case to find global extinction, the persistence time is the longest. In short, the level of synchrony between subpopulation is stronger, metapopulation is easier to find global extinction. Make all subpopulations synchronize is the easiest way at which disease goes to extinct.

#### 4.3.2 Global persistence when $\varphi_{max}$ alters

In this part, each Kaplan-Meier survival curve of the global disease persistence time in a metapopulation for each value  $\varphi_{max}$  is parametrized as rate by the survival regression model. Depending on the base of the persistence time caused by the phase difference in the metapopulation of two subpopulations, we are going to exploit metapopulations of many subpopulations. We use the parametric survival model to estimate this global persistence with confidence interval 95%. The result is shown as following figure 6.

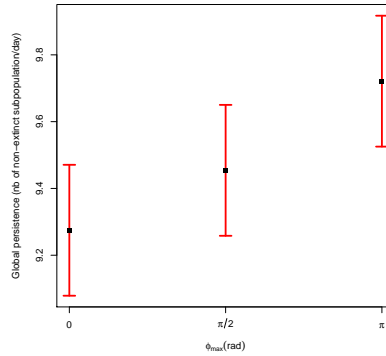


Figure 6: Global disease persistence in the metapopulation of eight subpopulations after 100 different simulations  $N=3*10^5$ , coupling rate  $\rho = 0.1$ . Here, with 95% confidence interval, these intervals are limited by lower and upper confidence limits.

This figure 6 points out to us that the distance of the estimated scales is quite far to each other. The global persistence in the metapopulation rises when  $\varphi_{max}$  runs from 0 to  $\pi$ . The phase difference strongly influences both disease persistence time and global disease persistence probability. In addition to the global persistence, we also gather the global extinction rate for this metapopulation of eight subpopulations as follows :



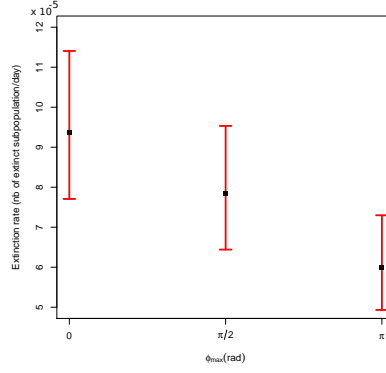


Figure 7: Global extinction rate in the metapopulation of eight subpopulations after 100 different simulations  $N=3 \cdot 10^5$ , coupling rate  $\rho = 0.1$ . Here, with 95% confidence interval, these intervals are limited by lower and upper confidence limits.

The global extinction rates of  $\varphi_{max}$  are in an inverse of the global persistence. We see that the extinction rate reduces when the degree of asynchrony augments. So in order to destroy infectious diseases, we need to make subpopulations be in synchrony over long time. The asynchrony between subpopulations is the main reason to respond very familiar question why has the infectious disease been never extinct.

#### 4.3.3 Influence of demographic parameters on persistence of infectious diseases

**Population size of subpopulation** In the metapopulation of 06 subpopulations, we implement experiences with different population sizes of subpopulation. We performe 100 different simulation for the metapopulation of 06 subpopulations in which all subpopulation has the same population size  $N$ . We set  $N$  from 5000 to 500000 individuals. The result (Figure 8) affirms that the population size influences strongly the global persistence time of an infectious disease in a metapopulation. The number of individuals in a subpopulation increases, so the global persistence of disease increases also.

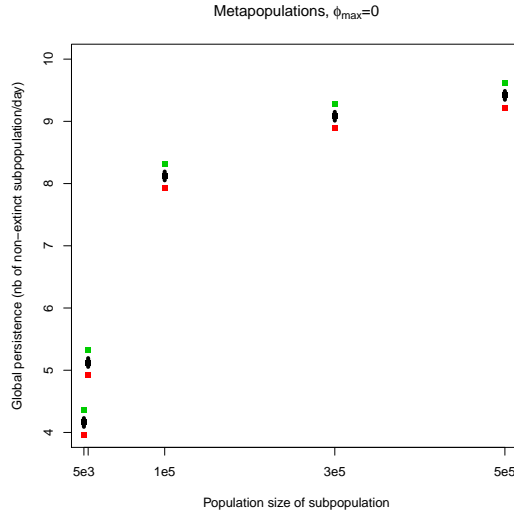


Figure 8: Global persistence in the metapopulation of six subpopulations after 100 different simulations. The population size of subpopulation is in the set  $\{5000, 10000, 10^5, 3 \cdot 10^5, 5 \cdot 10^5\}$ . Here, with 95% confidence interval, these intervals are limited by lower and upper confidence limits.

## Number of subpopulation in a metapopulation

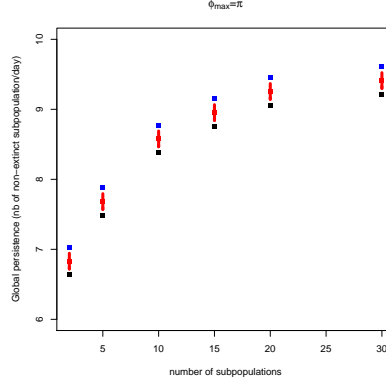


Figure 9: Global persistence of disease in the metapopulation of multi-subpopulations after 100 different simulations. The number of subpopulations alters in the set  $\{2, 5, 10, 15, 20, 25, 30\}$ . Here, with 95% confidence interval, these intervals are limited by lower and upper confidence limits.

In addition to the result of the population size, here we are going to explore influence of the number of subpopulation in a metapopulation on disease persistence of this metapopulation. We set first all metapopulation is the same population size  $N = 10^5$  and  $\varphi_{max} = \pi$  and the coupling rate  $\rho = 0.001$  then we change the number of subpopulation in metapopulation from three to 30. We obtain the same result as when the population size augments. The persistence probability scales directly the number of subpopulation in a metapopulation.

**Coupling force** According to Keeling(2008), due to dispersal rate  $\rho$ , the persistence time of metapopulation is considered as a function of dispersal rate. In order to affirm this supposition, here we change coupling rate from weak to strong in a metapopulation of five subpopulations with the population size of each subpopulation  $N = 10^5$ . The dispersal rate  $\rho$  is divided into three intervals. These are low, intermediate and high coupling rate intervals. In each interval, we choose some coupling rates that highlight the coupling strength among subpopulations in metapopulation. We have the result as follows (figure 10).

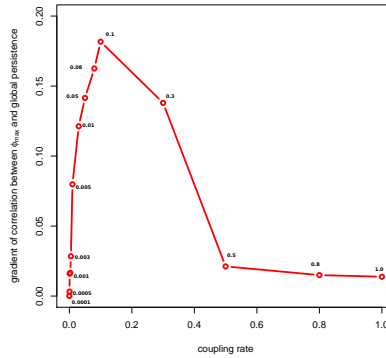


Figure 10: Correlation between coupling rate and gradient of level of synchrony and persistence probability in the metapopulation of five subpopulation. Here, the coupling rate  $\rho$  is in 0.0001, 0.0005, 0.001, 0.003, 0.005, 0.01, 0.3, 0.5, 0.8, 1.0, the level of asynchrony  $\varphi_{max}$  in  $0, \pi/2, \pi$  and the population size of each subpopulation  $N=10^5$ .

When the coupling rate is small from 0.0001 to 0.003, the gradient of the correlation between  $\varphi_{max}$  and the global persistence increases very slowly. However, the persistence probability augments in a sudden way when the coupling

rate changes from 0.005 to 0.1. Lastly, the gradient strongly decreases when the coupling rate is so robust from 0.3 to 1.0. Based on this figure, the global disease persistence in a metapopulation is one humped function for the coupling rate. The medium coupling rate (from 0.005 to 0.1) maximizes disease persistence in metapopulation.

## 5 Conclusion and perspective

We successfully built a version for the susceptible-infected-recovered stochastic metapopulation model. The infection rate  $\lambda_i$  for *subpopulation<sub>i</sub>* portrayed all effects inside as well as outside on disease transmission chain between individuals in the same subpopulation or among subpopulations. Moreover, our metapopulation model became more detailed when we brought seasonality in metapopulation model to create periodic transmission in year that here highlights seasonal change as well as school period of children. We have metapopulation model with different contact rates. This is more complex model than any used metapopulation model. We sketched successfully in-phase and sometime out-of-phase (“antiphase”) models across suburbs of He’s 2003 [8]. In addition, the results about the persistence of infectious diseases are in agreement Rozhnova(2012) [18], Heino in 1997 [10], Huffaker(1958) [12], Holyoak and Lawler(1996) [11], and Yaari et al. (2012) [21] when they exhaustively explored the disease persistence behavior of many different metapopulation models.

In order to continue my thesis, we will exploit the global persistence and the disease transmission among subpopulations under a new shape of metapopulation in epidemiology. It is the gravity model in epidemiology. This model is a very simple model, and can be used to explain the spatial epidemiologic dynamics. We says it simply that the strength of coupling between any two populations depends on the size of these two populations and the distance between them (so this model is quite similar to Newton’s law of universal gravitation, the attraction between two bodies depends on the masses of the bodies and the distance between the bodies). In epidemiology, we will call the “mass” the population size. Then, we set a gravity metapopulation model with the different positions and the different population sizes of subpopulations. Finally, we will exploit the disease transmission in the gravity metapopulation model.

One more main work in my thesis, it is the optimization of the vaccination policies. We set it in the last part of my thesis, because first of all, we must deeply exploit the actual nature of the infectious disease transmission in the different disease model, then we are going to have a good vaccination policy for a metapopulation.

## Manuscript :

T.C.G. Tran, M.Choisy, J.D. Zucker, Quantifying the effect of synchrony on the persistence of infectious diseases in a metapopulation.

## References

- [1] S. Altizer, A. Dobson, P. Hosseini, P. Hudson, M. Pascual, and P. Rohani. Seasonality and the dynamics of infectious diseases. *Ecol Lett*, 9(4):467–484, Apr 2006.
- [2] R. M. Anderson and R. M. May. *Infectious Diseases of Humans: Dynamics and Control*. Oxford University Press, 1992.
- [3] B. Bolker and B. Grenfell. Space, persistence and dynamics of measles epidemics. *The Royal Society*, 348:309–320, 1995.
- [4] B. M. Bolker and B. T. Grenfell. Impact of vaccination on the spatial correlation and persistence of measles dynamics. *Proc Natl Acad Sci U S A*, 93(22):12648–12653, Oct 1996.
- [5] D. T. Gillespie. Exact stochastic simulation of coupled chemical reactions. *The journal of physical chemistry*, 81(25):2340–2361, 1977.
- [6] B.T. Grenfell, B. M. Bolker, and A. Klegzkowski. Seasonality and extinction in chaotic metapopulation. *The royal society*, 259:97–103, 1995.
- [7] I. Hanski. Metapopulation dynamics. *Nature*, 396, 1998.

- [8] D. He and L. Stone. Spatio-temporal synchronization of recurrent epidemics. *Proc Biol Sci*, 270(1523):1519–1526, Jul 2003.
- [9] healthmap.org. Measles reemerges in vietnam, 2014.
- [10] M. Heino, V. Kaitala, E. Ranta, and J. Lindstrom. Synchronous dynamics and rates of extinction in spatially structured populations. *The Royal Society*, 264:481–486, 1997.
- [11] M. Holyoak and S. P. Lawler. Persistence of an extinction-prone predator-prey interaction through metapopulation dynamics. *Ecology*, pages 1867–1879, 1996.
- [12] C. B. Huffaker. Experimental studies on predation: dispersion factors and predator-prey oscillations. *Hilgardia*, 27:343–383, 1958.
- [13] M. J. Keeling and B. T. Grenfell. Understanding the persistence of measles: reconciling theory, simulation and observation. *Proc Biol Sci*, 269(1489):335–343, Feb 2002.
- [14] M. J. Keeling and P. Rohani. *Modeling Infectious Diseases in humans and animals*. Princeton University Press, 2008.
- [15] R. Levins. Some demographic and genetic consequences of environmental heterogeneity for biological control. *Bulletin of the Entomological Society of America*, 15:237–240, 1969.
- [16] A. L. Lloyd. Realistic distributions of infectious periods in epidemic models: changing patterns of persistence and dynamics. *Theor Popul Biol*, 60(1):59–71, Aug 2001.
- [17] E. Renshaw. *Modelling biological populations in space and time*, volume 11. Cambridge University Press, 1993.
- [18] G. Rozhnova, A. Nunes, and A. J. McKane. Phase lag in epidemics on a network of cities. *Phys Rev E Stat Nonlin Soft Matter Phys*, 85(5 Pt 1):051912, May 2012.
- [19] T. M. Therneau. *A Package for Survival Analysis in S*, 2014. R package version 2.37-7.
- [20] WHO. Reported measles cases with onset date from oct 2013 to mar 2014, 2014.
- [21] G. Yaari, Y. Ben-Zion, N. M. Shnerb, and D. A. Vasseur. Consistent scaling of persistence time in metapopulations. *Ecology*, 93(5):1214–1227, May 2012.
- [17] <http://microbiology.mtsinai.on.ca/faq/transmission.shtml>
- [18] [http://en.wikipedia.org/wiki/Epidemic\\_model](http://en.wikipedia.org/wiki/Epidemic_model)